Compressed Sensing of Fetal Electrocardiogram Signals Based on Joint Block Multi-Orthogonal Least Squares Algorithm

Xiang Jianhong, Wang Cong, Wang Linyu

Abstract—With the rise of medical IoT technologies, Wireless body area networks (WBANs) can collect fetal electrocardiogram (FECG) signals to support telemedicine analysis. The compressed sensing (CS)-based WBANs system can avoid the sampling of a large amount of redundant information and reduce the complexity and computing time of data processing, but the existing algorithms have poor signal compression and reconstruction performance. In this paper, a Joint block multi-orthogonal least squares (JBMOLS) algorithm is proposed. We apply the FECG signal to the Joint block sparse model (JBSM), and a comparative study of sparse transformation and measurement matrices is carried out. A FECG signal compression transmission mode based on Rbio5.5 wavelet, Bernoulli measurement matrix, and JBMOLS algorithm is proposed to improve the compression and reconstruction performance of FECG signal by CS-based WBANs. Experimental results show that the compression ratio (CR) required for accurate reconstruction of this transmission mode is increased by nearly 10%, and the runtime is saved by about 30%.

Keywords—Telemedicine, fetal electrocardiogram, compressed sensing, joint sparse reconstruction, block sparse signal.

I. INTRODUCTION

WBANs can receive real-time FECG dynamic data via smartphones. Usually, its real-time data collection and computation make mobile phones consume a lot of energy [1]. Using CS technology [2] can avoid sampling large amounts of redundant information and reduce the complexity and computation time of data processing. Thereby, the power consumption of the device can be reduced. This application is widely used in the prevention of fetal Congenital Heart Disease (CHD) [3], so the research on the FECG estimation algorithm has become a hot issue in the past two years.

Compared with Discrete Wavelet Transform (DWT)-based compression, CS-based WBANs systems exhibit poor compression performance and signal reconstruction quality [4]. Therefore, improving the performance of CS-based signal compression and reconstruction can better facilitate the application of WBANs systems. FECG signals are embedded in strong noise and artifacts caused by maternal ECG, instrument noise, and abdominal EMG [5], so the detection of FECG signals usually uses multiple channels. It can be seen from Fig. 1 that the FECG signals of different channels have similar structural information. After wavelet transform, the FECG signals of different channels show joint features and

block sparse features in the wavelet domain, that is, the FECG signals of different channels are similar in distribution but values are different, and the non-zero terms of the signal appear in the block, as shown in Fig. 2. Therefore, for optimal performance, FECG compression techniques that exploit the joint properties of multiple channels and block sparse properties should be considered.
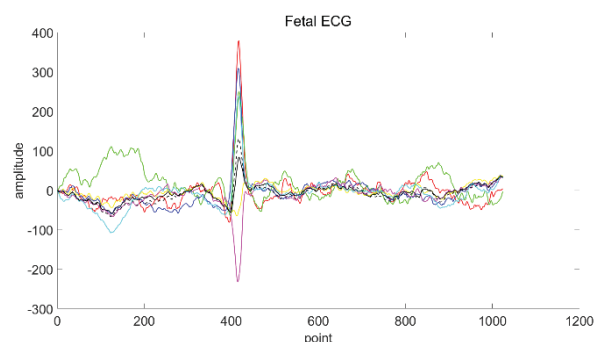

Fig. 1 8-channel FECG signal

In [6], the authors proposed a weighted L1,2 minimization (WL12M) method to reconstruct MECG and FECG signals. It utilizes inter-channel priors and multi-source priors in the wavelet domain for MECG and FECG signal reconstruction, proving that utilizing FECG inter-channel correlation can improve reconstruction performance. This algorithm is an optimization algorithm, which can be accurately reconstructed under a high CR, but the running time is too long to meet the real-time requirements of the WBANs system. Reference [7] proposed a JBSM based on the joint feature of the signal and the block sparse feature. The joint block sparse reconstruction algorithm can be used to reconstruct the signal conforming to the model, with improved accuracy and running time. The author proposes the JBOMP algorithm, but this algorithm is only a simple improvement of the traditional BOMP algorithm. When the CR is high, it cannot reconstruct signals accurately. Reference [8] proposes a block sparse MECG compression scheme, which effectively utilizes the spatiotemporal correlation and multi-scale information of the wavelet domain MECG data, and proposes the WJCS algorithm, which is superior to the WL12M algorithm in reconstruction performance and running time, but the time consumption of the

Xiang Jianhong, Wang Cong, and Wang Linyu are with Harbin Engineering University, College of Information & Communication Engineering, Harbin 150001, Heilongjiang, Peoples R China and with Key Laboratory of Advanced Ship Communication and Information Technology, Harbin Engineering University, China (e-mail: wangcong98@hrbeu.edu.cn).

World Academy of Science, Engineering and Technology
International Journal of Information and Communication Engineering
Vol:17, No:6, 2023

algorithm is still too large. Reference [9] proposed a non-iterative ECG reconstruction (CSNet) algorithm based on deep learning technology, which combines CNN and LSTM to directly learn the mapping relationship between measured values and original signals. Under high CR, the signal reconstruction accuracy and reconstruction speed are better than traditional reconstruction algorithms. However, deep learning methods require extensive training, consume a lot of resources, and are difficult to implement in hardware.
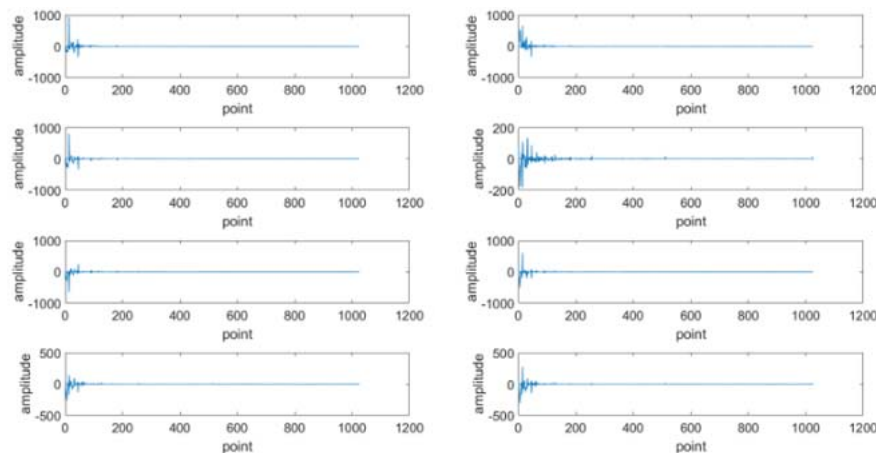

Fig. 2 DWT domain waveform of FECG signal

Different wavelet base types have different performances for the sparse representation of different signals, but the current research on the sparse representation of FECG signals is not enough. Qu et al. [10] compared the reconstruction errors of several wavelet bases and believed that the reconstruction error of the coif5 wavelet base was relatively small. However, this conclusion only comes from the simulation results of the same ECG data and cannot be applied to other situations. The simulation only selects 6 wavelet bases for comparison, ignoring the effects of the changes in the internal parameters of the wavelet bases. Mishra et al. [11] studied different wavelet bases and gave the optimal wavelet bases under several CRs. However, the obtained wavelet-based sparse representation performance results are only applicable to specific conditions. When testing with other ECG signals, or changing the CR and recovery algorithm, the reconstruction accuracy of the signal will be affected.

For multi-channel FECG signals, a JBMOLS algorithm based on JBSM is proposed. A comparative experiment is set up for all kinds of wavelet bases and measurement matrices, and the optimal wavelet bases and optimal measurement matrices suitable for these FECG signals are obtained, which provides a practical basis for practical applications.

A. Contribute

◆ A JBMOLS algorithm is proposed. It utilizes the joint features and block sparse characteristics of FECG signals, uses the block orthogonal projection method to solve the problem of low atomic selection accuracy for block sparse signals, and uses multiple selections and backtracking to solve the problem of too many algorithm iterations and long running time.

◆ A WBANs simulation experiment system is established. First, the compression performance of 52 wavelet bases and 7 measurement matrices for different combinations of FECG signals is verified, and the most suitable Rbio5.5 wavelet and Bernoulli measurement matrices for FECG signals are obtained. On the other hand, it is verified that the reconstruction ability and algorithm running time of the JBMOLS algorithm are superior to similar algorithms.

◆ Based on the JBMOLS algorithms, FECG signals compression and transmission mode is proposed, which combines Rbio5.5 wavelet, Bernoulli measurement matrix, and JBMOLS algorithm. Its performance was proved by experiments, which improved the compression and reconstruction performance of CS-based WNANs systems.

B. Thesis Notation

The notations covered in this paper are summarized as follows: For all $n \in \mathbb{N}$, we define the set $\{1, 2, \ldots, n\}$ as Ω. For $T \in \Omega$, $|T|$ represents the T absolute value. The vector spaces of n tuples and $m \times n$ matrices are denoted by $\mathbb{R}^n$ and $\mathbb{R}^{m \times n}$, respectively. We will use $A \in \mathbb{R}^{m \times n}$ to represent matrices. The i-th column of the matrix A is denoted by a_i, its submatrix is denoted by A_I, where I denotes the column index of the atoms in the submatrix, and $I \subseteq \Omega$. A^k represents the value A of the k-th iteration. For any subspace S belongs to $\mathbb{R}^m$, P_S represents the projection on S. $x[\bullet]^T$ represents the transpose of a vector x. We denote the measurement matrix by $\Phi \in R^{N \times M}$. $\mathfrak{R}(A)$ is the spatial extent spanned by the column A. $\mathfrak{R}(\Phi)$ indicates the range space spanned by the column of Φ, for which φ_i is the i-th column of Φ.

II. BACKGROUND

A. Compressed Sensing

CS theory breaks through the requirements of Nyquist sampling theorem, compresses and samples signals with a sampling number far lower than traditional sampling techniques. CS proves that it is possible to accurately

World Academy of Science, Engineering and Technology
International Journal of Information and Communication Engineering
Vol:17, No:6, 2023

reconstruct signals from signals with some sparse coefficients, reducing the storage and transmission requirements of the data acquisition system.

First, we assume that the original signal $x = x(n), n \in [1,2,\cdots,N]$ is a one-dimensional discrete signal. If given a set of standard orthonormal basis $\Psi = \{\psi_1, \psi_2, \cdots, \psi_n\}$, such as (1):

$$x = \sum_{k}^{N} \alpha_k \psi_k = \Psi\alpha \qquad (1)$$

ψ_k is the column vector of Ψ, the coefficient is $\alpha_k = \langle x, \psi_k \rangle$, the representation of the signal x in the Ψ transform domain is α. x is the $N \times 1$ matrix, Ψ is the $N \times N$ matrix, α is the $N \times 1$ matrix. If the signal x has only K non-zero values in the Ψ transform domain, or only K large coefficients ($K \ll N$), the x signal is considered to be sparse, and the signal x can be represented by K large coefficients.

The theory of CS requires that the signal is sparse, or it is sparse after a certain transformation, which is also called the prior condition of CS. Assuming that the signal x is K sparse on the orthonormal basis $\Psi = \{\psi_1, \psi_2, \cdots, \psi_n\}$, a measurement matrix Φ with low correlation with the sparse basis Ψ can be selected to observe the signal, which Φ is a $M \times N$ matrix, and $K \ll M \ll N$. The measured value y is obtained, in which y is $M \times 1$ the matrix, such as (2):

$$y = \Phi x = \Phi\Psi\alpha \qquad (2)$$

Finally, the CS utilizes the small number of measurements y and measurement matrices Φ to recover the signal x, solving the optimization problem under the 0-norm, such as (3):

$$\begin{cases} \tilde{\alpha} = \arg\min \|\alpha\|_0 \\ s.t. \ y = \Phi x = \Phi\Psi\alpha \end{cases} \qquad (3)$$

The only deterministic solution α can be obtained. However, the optimization problem under 0-norm is an NP-hard non-convex optimization problem, so the l_1-norm is usually used to replace the non-convex optimization problem, such as (4):

$$\begin{cases} \tilde{\alpha} = \arg\min \|\alpha\|_1 \\ s.t. \ y = \Phi x = \Phi\Psi\alpha \end{cases} \qquad (4)$$

This transforms the problem in the equation into a convex optimization problem, which can be transformed into a linear programming problem to solve, and the signal x can be obtained by substituting into (1).

B. Joint Block Sparse Model

Traditional CS only considers the sparse signal with the most K non-zero elements, and does not involve the structure of the signal itself. In practical problems, some sparse signals will exhibit a special structure with non-zero elements appearing in blocks. Such a signal is called a block sparse signal. Given a block $I = \{d_1, d_2, \ldots, d_N\}$, a block sparse signal $x \in R^N$ can be described as:

$$x = [x_1, \ldots, \underbrace{x_{d_1}}_{x[1]}, x_{d_1}, \ldots, \underbrace{x_{d_1+d_2}}_{x[2]}, \ldots, \underbrace{x_{m-d_N+1}}_{x[N]}, \ldots, x_m]^T \quad (5)$$

where $x[i]$ is the i-th block in the source signal and d_i is the size of each block.

Correspondingly, the measurement matrix $\Phi \in R^{N \times M}$ can also be described in the following form:

$$\Phi = [\varphi_1, \ldots, \underbrace{\varphi_{d_1}}_{\Phi[1]}, \varphi_{d_1}, \ldots, \underbrace{\varphi_{d_1+d_2}}_{\Phi[2]}, \ldots, \underbrace{\varphi_{m-d_N+1}}_{\Phi[N]}, \ldots, \varphi_m]^T \quad (6)$$

The CS mathematical model of block signals can be described as

$$y = \sum_{i=1}^{N} \Phi[i]x[i] \qquad (7)$$

For a given block I, the signal x has at most K non-zero block, as

$$\|x\|_{2,0} = \sum_{i=1}^{N} I(\|x[i]\|_2) \le K \qquad (8)$$

It is called a K sparse block signal, where the $I(\bullet)$ is the indicator function, satisfying

$$I(x) = \begin{cases} 1 & x \ne 0 \\ 0 & x = 0 \end{cases} \qquad (9)$$

In fact, at that time $d_i = 1(i = 1,2,\ldots,N)$, the block sparse signal model degenerated into the traditional sparse signal model.

When a group of block sparse signals has joint features, that is the non-zero coefficients of the group of signals appear in the same position, only the values are different, the signal model becomes the block sparse signal model with joint features as shown in Fig. 3, which is called JBSM [7]. In Fig. 3, $x(n_a)$ represents the n_a-th signal in a set of joint signals, $x_N()$ represents the N-th block in the block sparse signal, with black dots representing values there and white dots representing zeros there. It can be observed that each channel of the multi-channel FECG signals after wavelet transformation has joint features, and each channel signal has the block sparse feature, which conforms to JBSM and can be reconstructed by the joint block sparse algorithm.

III. WAVELET SPARSE TRANSFORM AND MEASUREMENT MATRIX

A. Wavelet Sparse Transform

There are 6 kinds of wavelet basis for sparse basis, considering parameter changes, there are 52 kinds in total: $Haar$; $Dbn(n = 2\sim10)$; $Symn(n = 2\sim8)$; $Coifn(n = 1\sim5)$; $Bior(n_r.n_d)$ $(n_r = 1, n_d = 1, 3, 5; n_r = 2, n_d = 2, 4, 6, 8; n_r = 3, n_d = 1, 3, 5, 7, 9; n_r = 4, n_d = 4; n_r = 5, n_d = 5;$

World Academy of Science, Engineering and Technology
International Journal of Information and Communication Engineering
Vol:17, No:6, 2023

$n_r = 6$, $n_d = 8$); $Rbio(n_r.n_d)$ ($n_r = 1$, $n_d = 1, 3, 5$; $n_r = 2$, $n_d = 2$, 4, 6, 8; $n_r = 3$, $n_d = 1, 3, 5, 7, 9$; $n_r = 4$, $n_d = 4$; $n_r = 5$, $n_d = 5$; $n_r = 6$, $n_d = 8$).
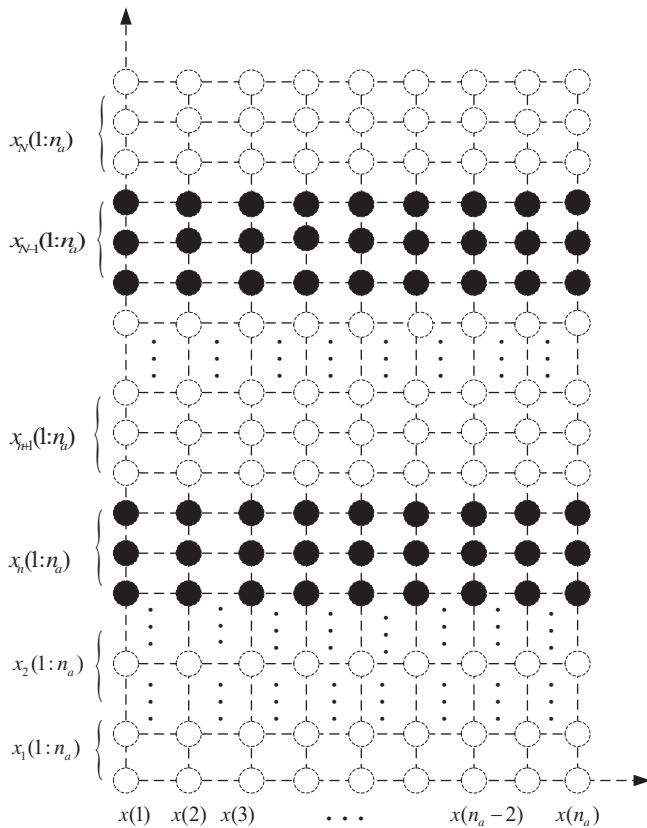

Fig. 3 Schematic diagram of the JBSM

In this paper, a WBANs simulation experiment system is built, which can simulate the signal transmission process. We select the FECG data (signal 01) in the OSET Fetal ECG database [12] as the signal sample, and select a segment with a length of 1024 sampling points as the sample in this experiment. The measurement matrix is selected as the Bernoulli matrix, and the recovery algorithm is the Orthogonal Matching Pursuit (OMP) algorithm [13]. Using 52 kinds of wavelet bases as experimental variables, 8 channels of FECG signals were simulated under 15 kinds of CR. Each group of experiments was repeated 10 times, and the average value was taken as the experimental data, for a total of 62,400 experiments.

This paper adopts CR, Percent root means square difference (PRD) [14], and Reconstruction rate as performance evaluation metrics. CR describes the effect of compressed data, that is, the ratio of the reduced length of the compressed signal to the length of the original signal. The higher the CR, the more difficult the reconstruction. Let the length of the original signal is N and the number of measurement points is M, then

$$CR = \frac{N-M}{N} \times 100\% \qquad (10)$$

PRD describes the difference between the reconstructed signal and the original signal, set x as the original signal and $\hat{x}$ as the reconstructed signal, then

$$PRD = \frac{\|x - \hat{x}\|_2}{\|x\|_2} \times 100\% \qquad (11)$$

Reconstruction rate describes the success rate of signal reconstruction in multiple experiments. It is generally considered that $PRD <= 10\%$ is the ideal reconstructed signal, the test was successful, then

$$Reconstruction\ rate = \frac{Success\ times}{Total\ times} \qquad (12)$$

In experiments, $PRD <= 10\%$ reconstruction will be considered a success. If multiple groups of wavelet bases are successfully reconstructed, the first three groups with the smallest PRD are selected and recorded in the table. If all wavelet bases fail to be reconstructed successfully, we select a set of records with the smallest PRD to enter the table. The experimental results are shown in Table I. It can be seen from the analysis that the influence of different wavelet bases on the reconstruction effect will change due to the change of the CR, and the Rbio5.5 wavelet has the best sparse representation effect on FECG signals under different CRs.

B. Measurement Matrix

The observation matrix needs to satisfy the Restricted equidistant property (RIP), so that the original signal can be recovered with high probability during the reconstruction stage [15]. The RIP criterion is shown in (13):

$$(1 - \zeta_S)\|X\|_{l_2}^2 \leq \|\Phi X\|_{l_2}^2 \leq (1 + \zeta_S)\|X\|_{l_2}^2 \qquad (13)$$

where: ζ_S is the Restricted Isometric Constant (RIC) [16], required $0 \leq \zeta_S \leq 1$.

We selected signal01 in the OSET fetal ECG database as the signal sample, and the fragment with a length of 256 sampling points are selected as the sample of this experiment.

We selected the Gaussian random matrix, Bernoulli matrix, Circulant matrix, Partial Hadamard matrix, Toeplitz matrix, Partial Fourier matrix and Sparse random matrix as the measurement matrix of the research object. The classical Orthogonal matching pursuit algorithm (OMP) is used to complete the signal reconstruction.

The relationship between the observation value M and the Reconstruction rate under different observation matrices is drawn. Each group of experiments is repeated 100 times, and the average value is taken as the experiment data, as shown in Fig. 4. It can be seen from Fig. 4 that the Reconstruction rate increases significantly as M increases (the CR decreases). For different wavelet sparsity, the reconstruction performance of the Gaussian measurement matrix and Bernoulli measurement matrix is better than other matrices, while the Bernoulli measurement matrix is slightly earlier than Gaussian matrix and reaches 100% reconstruction ability, and the Bernoulli observation matrix elements are ± 1, which is easier to

World Academy of Science, Engineering and Technology
International Journal of Information and Communication Engineering
Vol:17, No:6, 2023

implement in hardware.

TABLE I
WAVELET BASIS WITH BETTER PERFORMANCE UNDER VARIOUS CRs

CR	FECG1	FECG2	FECG3	FECG4	FECG5	FECG6	FECG7	FECG8
10%	**rbio5.5**	**rbio5.5**	coif4	db9	bior1.5	db9	sym8	**rbio5.5**
	coif5	db10	sym6	db10	db10	coif4	db9	coif5
	bior2.8	db9	**rbio5.5**	**rbio5.5**	db9	sym7	bior2.8	db9
15%	**rbio5.5**	**rbio5.5**	coif4	db9	**rbio5.5**	**rbio5.5**	**rbio5.5**	**rbio5.5**
	bior2.8	coif5 db10	**rbio5.5**	**rbio5.5**	db9	sym7	coif4	bior2.8
	coif5		sym8	db10	coif4	db8	bior2.8	db7
20%	**rbio5.5**	**rbio5.5**	**rbio5.5**	**rbio5.5**	**rbio5.5**	**rbio5.5**	**rbio5.5**	**rbio5.5**
	bior2.8	bior2.8	bior2.8	bior3.9	bior3.9	bior2.8	bior2.8	bior2.8
	bior3.9	bior2.6	bior3.9	db9	bior2.8	bior3.9	bior3.9	bior2.6
25%	**rbio5.5**	**rbio5.5**	**rbio5.5**	bior3.9	bior3.9	**rbio5.5**	bior2.8	**rbio5.5**
	bior2.8	bior3.9	bior3.9	bior2.8	**rbio5.5**	bior2.8	**rbio5.5**	bior3.9
	bior2.6	bior2.8	bior2.8	**rbio5.5**	bior3.7	bior3.9	bior3.9	bior2.8
30%	**rbio5.5**	bior3.9	bior3.9	bior3.9	bior3.9	**rbio5.5**	bior3.9	bior3.9
	bior3.9	**rbio5.5**	**rbio5.5**	**rbio5.5**	**rbio5.5**	bior3.9	**rbio5.5**	**rbio5.5**
	bior2.8	bior2.8	bior2.8	bior3.7	bior3.7	bior3.7	bior3.7	bior2.8
35%	**rbio5.5**	bior3.9	bior3.9	bior3.9	bior3.9	**rbio5.5**	bior3.9	bior3.9
	bior3.9	**rbio5.5**	bior2.8	bior3.7	**rbio5.5**	bior3.9	**rbio5.5**	**rbio5.5**
	bior3.7	bior2.8	bior3.7	**rbio5.5**	bior2.8	bior3.7	bior3.7	bior3.7
40%	**rbio5.5**	bior3.9	**rbio5.5**	bior3.7	bior3.9	bior3.7	**rbio5.5**	bior3.9
	bior2.8	**rbio5.5**	bior2.8	bior3.9	**rbio5.5**	**rbio5.5**	bior3.7	**rbio5.5**
	bior2.6	bior3.7	bior3.9	**rbio5.5**	bior3.7	bior3.9	bior2.8	bior3.7
45%	**rbio5.5**	**rbio5.5**	**rbio5.5**	**rbio5.5**	**rbio5.5**	**rbio5.5**	**rbio5.5**	**rbio5.5**
	bior2.8	bior3.9	bior3.7	bior3.7	bior3.9	bior3.7	bior2.8	bior2.6
	bior2.6	bior3.7	bior3.9	bior2.8	bior2.8	bior3.9	bior3.7	bior2.8
50%	**rbio5.5**	**rbio5.5**	**rbio5.5**	**rbio5.5**	**rbio5.5**	**rbio5.5**	**rbio5.5**	**rbio5.5**
	bior2.8	bior3.9	bior3.9	bior3.7	bior3.9	bior2.8	bior2.8	bior2.8
	bior2.6	bior3.7	bior2.6	bior2.6	bior2.8	bior3.9	bior2.6	bior2.6
55%	**rbio5.5**	rbio5.5	**rbio5.5**	**rbio5.5**	**rbio5.5**	bior3.9	**rbio5.5**	**rbio5.5**
	bior2.8	bior2.8	bior3.9	bior2.8	bior3.9	**rbio5.5**	bior2.8	bior2.8
	bior2.6	bior3.9	bior3.5	bior2.6	bior2.8	bior2.8	bior2.6	coif5
60%	**rbio5.5**	**rbio5.5**	**rbio5.5**	**rbio5.5**	**rbio5.5**	**rbio5.5**	**rbio5.5**	**rbio5.5**
	bior2.6	bior2.8	bior2.8		bior2.8	bior3.7	bior2.8	bior2.8
	bior2.8	bior3.9	bior3.9		bior3.9	bior2.8	db7	bior2.6
65%	**rbio5.5**	**rbio5.5**	**rbio5.5**	**rbio5.5**	**rbio5.5**	**rbio5.5**	**rbio5.5**	**rbio5.5**
	bior2.8	bior2.8	bior2.8		bior1.5	bior2.8	coif5	coif5
	bior2.6	coif4	coif5		bior2.8	bior2.6	bior2.8	bior3.9
70%	**rbio5.5**	**rbio5.5**	**rbio5.5**	**rbio5.5**	**rbio5.5**	**rbio5.5**	**rbio5.5**	**rbio5.5**
	bior2.8		bior1.5		bior3.9	bior2.8		coif5
	bior2.6		bior2.8		bior2.8	bior2.6		
75%	**rbio5.5**	rbio5.5	**rbio5.5**	rbio5.5	**rbio5.5**	**rbio5.5**	rbio5.5	rbio5.5
			sym7			db10		
			bior1.5			coif3		
80%	bior1.5	**rbio5.5**	**rbio5.5**	**rbio5.5**	**rbio5.5**	**rbio5.5**	**rbio5.5**	**rbio5.5**

By comparing the Reconstruction rate of various wavelet bases on the original signal in Fig. 4, the influence of selecting different wavelet bases on signal reconstruction can be verified again. For example, the Rbio3.3 wavelet cannot achieve accurate reconstruction, while the Rbio5.5 wavelet achieves accurate reconstruction can be done with smaller M. Therefore, based on the above analysis, considering the realization of the embedded hardware system, the Rbio5.5 wavelet is used to construct the sparse.

IV. RECONSTRUCTION ALGORITHM

CS reconstruction algorithms are mainly divided into two categories: convex optimization algorithms and greedy algorithms. The reconstruction performance of the convex optimization algorithm is excellent, but the running time of the algorithm is much higher than that of the greedy algorithm. Greedy algorithms are mainly two different methods for the sparse reconstruction problem, one is the OMP algorithm, and the other is the Orthogonal Least Squares (OLS) algorithm [17]. The OMP means that in the process of atom selection, the atom with the largest inner product value is selected, that is, the most relevant atom; the OLS atom is selected in a different way. After orthogonal projection of all atoms, the atom with the smallest iteration residual is selected. Atoms are selected into the support set, and atoms to be selected in subsequent iterations must be combined with previously selected atoms to minimize the residual value. Compared with the OMP algorithm, the OLS algorithm can complete accurate reconstruction with less sparsity. However, the OMP algorithm only needs to perform the linear product of the summation Φ and r in each iteration to achieve atom selection, which is relatively simple; but the OLS requires $N - (t-1)$ orthogonal projection (N measures the number of matrix columns and the number t of iterations), and the computational complexity is high. It can be said that it consumes a certain amount of running time in exchange for a higher quality of reconstruction.
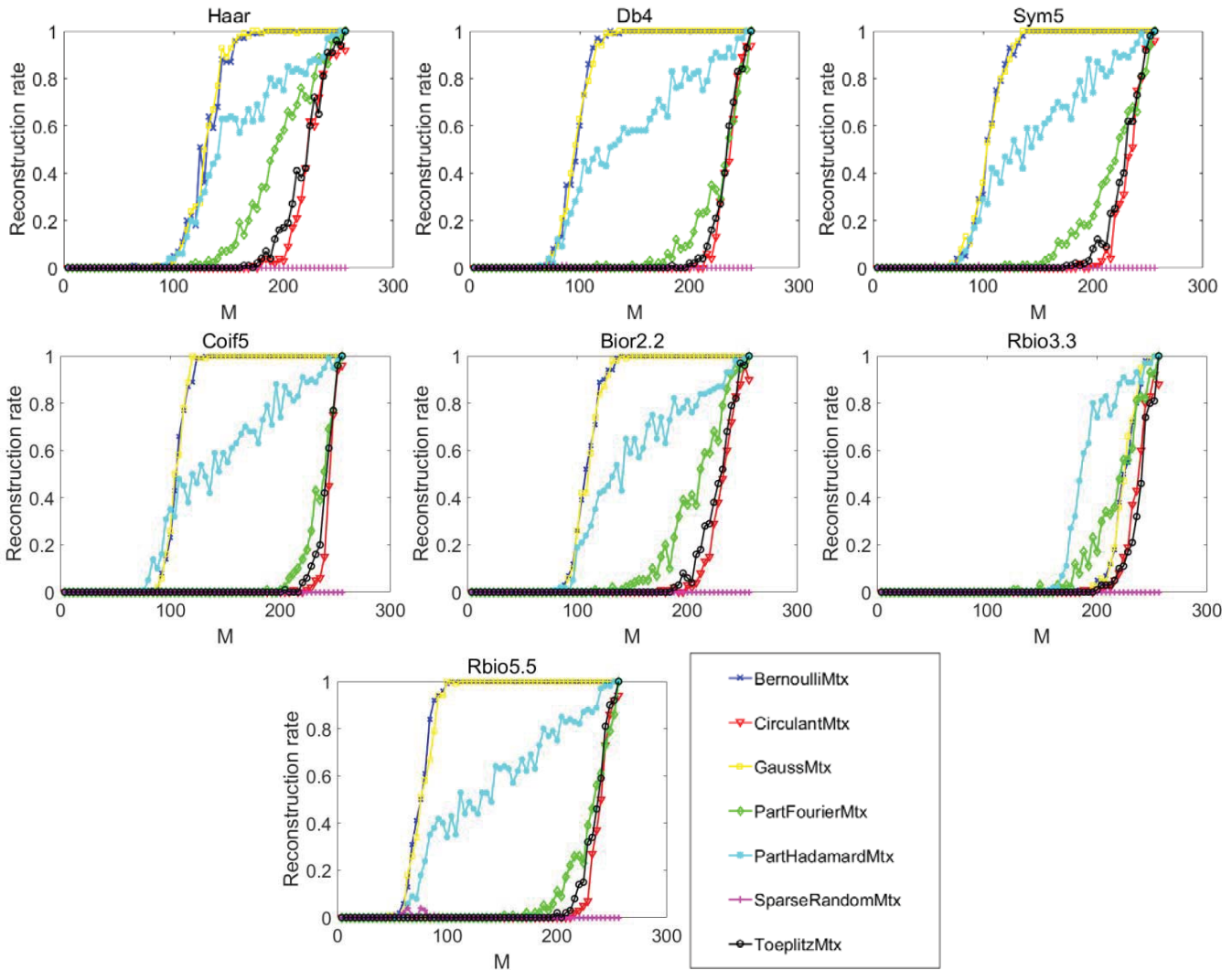
World Academy of Science, Engineering and Technology
International Journal of Information and Communication Engineering
Vol:17, No:6, 2023

Fig. 4 Reconstruction rate of FECG signal under different sparse wavelets and measurement matrices

A. Algorithm Introduction

The JBMOLS algorithm proposed in this paper utilizes the joint features of the signal itself and uses the atomic selection method of the Block Orthogonal Least Squares (BOLS) algorithm [18] to reconstruct the joint block sparse signal. Reference [19] proves that since the OLS algorithm has a more accurate advantage in atom selection, multiple atoms can be selected simultaneously when multiple atoms are selected into the support set. Based on this, the JBMOLS algorithm sorts all the atoms that meet the requirements according to the iterative residual, and selects multiple atomic blocks into the support set at a time.

Combined with the backtracking idea [20], when the block sparsity is greater than K, the optimal K atomic blocks are selected. In this way, the end of the JBMOLS algorithm is not limited by the block sparsity K, and the threshold method is used. When the residual of the reconstructed signal is less than a given threshold, the loop will be jumped out.

Before explaining the JBMOLS algorithm, we need to introduce the concept of subspace distance, which will be

applied to the identification step of the algorithm.

Theorem 1. (Subspace distance [21]) Define S_1 and S_2 as the subspace of R^m, let d_1 and d_2 be the dimension of S_1 and S_2 respectively. If $\{u_1,\ldots,u_{d_1}\}$ and $\{v_1,\ldots,v_{d_1}\}$ are the orthonormal basis of the S_1 and S_2 respectively, the distance $d(S_1,S_2)$ between the S_1 and S_2 is defined as follows:

$$d(S_1,S_2) = \sqrt{\max\{d_1,d_2\} - \sum_{i=1}^{d_1}\sum_{j=1}^{d_2}\left|\left\langle u_i, v_j\right\rangle\right|^2} \qquad (14)$$

The following is an analysis of the specific implementation process of the JBMOLS algorithm:

JBMOLS algorithm selects atoms according to the angle between the projection vector and the residual, that is, selects the column with the smallest subspace distance. The signal processed by the JBMOLS algorithm is a block sparse signal with joint features. At each iteration, the algorithm computes the subspace distance $D(n_a)$ of each atomic residual space $\Re(R^k)$ from the latest estimated space $\Re(P_{T^{k-1}\cup\{i\}}Y)$, and using

World Academy of Science, Engineering and Technology
International Journal of Information and Communication Engineering
Vol:17, No:6, 2023

the joint features of the Na group signals, computes the minimum value $u(l) = \sum_{i=1}^{Na} D(n_a)$. The joint sparse signal has the smallest subspace distance at this atom. Since the signal is a block sparse signal, it is necessary to find the best matching block of atoms rather than a single atom. When calculating $u(g) = \sum_{i=1}^{d} u(l)$, it will be evenly distributed $u(l)$ according to the block length d, and the atom with the smallest median value I corresponds to the smallest atomic block index. At each iteration, u(g) will be sorted and the top L most suitable atomic block indices will be selected into the support set. When the number of indices in the support set is greater than the sparsity K, the subspace distances of all atoms in the support set are calculated, and the optimal K atomic blocks are selected. Since the JBMOLS algorithm is not limited by the sparsity K, given the threshold ε and the maximum number of iterations$M$, when the residual error of the reconstructed signal is less than the given threshold or reaches the maximum number of iterations, it will jump out of the loop. In CS reconstruction, it is generally considered that the residual value $R < 10^{-6}$ reconstruction is successful, so it is assumed $\varepsilon = 10^{-6}$. The algorithm flow is shown in Table II.

B. Algorithm Complexity Analysis

According to the analysis of the literature [22], it can be seen that the calculation amount of BOMP algorithm to calculate a group of n_a signals is about $O(n_a kMP)$, and the calculation amount of BOLS algorithm to calculate a group of signals is about $O(n_a kLS)$. Because the OLS algorithm is more time-consuming, the $O(n_a kMP) < O(n_a kLS)$. Reference [22] points out that the calculation amount of the JBOMP algorithm is$O(n_a kMP)$, but due to the difference in the reconstruction of the sub-blocks of the algorithm, the calculation amount will be smaller than that of BOMP, $O(n_a kMP)_{JBOMP} < O(n_a kMP)_{BOMP} < O(n_a kLS)$. Since the JBMOLS algorithm selects L atoms at a time, the number of iterations becomes the original $1/L$ and the computational complexity is $O((n_a k/L)LS)$. So, we get the algorithm complexity comparison as $O((n_a k/l)LS) < O(n_a kMP)_{JBOMP} < O(n_a kMP)_{BOMP} < O(n_a kLS)$.

C. FECG Signal Reconstruction Experiment

Through the analysis in the previous sections, we propose a FECG signal compression transmission mode which combines Rbio5.5 wavelet, Bernoulli measurement matrix and JBMOLS algorithm. In order to verify the effect of this transmission method, the following experiments are carried out on the WBANs simulation experimental system. In the experiment, the FECG data (signal 01) in the OSET Fetal ECG database were selected as the signal sample, and a segment with a length of 512 sampling points was selected as the sample of this experiment. We select WL12M algorithm and BOLS, BOMP, JBOMP as sparse recovery algorithms. The performance indicators are CR and Reconstruction rate. CR is selected as the sampling interval 1.5% in the range of 62.5%~85%. The reconstruction ability and running time of different algorithms are compared, and the simulation is performed 1000 times. It is considered that PRD <= 10% indicates that the reconstruction is successful, and the Reconstruction rate is counted as the success rate, and the time average is taken.

TABLE II
JBMOLS ALGORITHM

Inputs:	Measurement data $Y \in \mathbb{R}^{m \times N}$, Measurement matrix $\Phi \in \mathbb{R}^{m \times n}$ Sparsity $K \in \mathbb{N}$, Block Length $d \in \mathbb{N}$, Number of Choices L
Initialization:	Reconstruction results $X^0 = 0$, Support sets $T^0 = \emptyset$, Residuals $R^0 = Y$, Thresholds $\varepsilon = 10^{-6}$,Iterations $h = 0$, Maximum iterations number M, Number of atoms $t = 0$
While	$t \le K$ or $R^h < \varepsilon$ or $h < M$ do $t = t + L$ $h = h + 1$ $D^h(n_a) = \underset{i \notin T^{h-1}}{\operatorname{argmin}} d(\Re(Y), \Re(P_{T^{h-1} \cup \{i\}} Y))$ $I^h = \underset{I:I \subset \Omega \setminus I^{h-1}, |I|=L}{\operatorname{argmin}} \sum_{i=1}^{d} \sum_{j=1}^{Na} D^h(n_a)$ $T^h = T^{h-1} \cup \{(I^h - 1)d + 1 : I^h d\}$ $X^h = \underset{U:supp(U) \subseteq T^h}{\operatorname{argmin}} \|Y - \Phi U\|_F$ $R^h = Y - \Phi X^h$
End While	
	$t > K$ or $h < M$ or $R^h < \varepsilon$ do $D^h(n_a) = \underset{i \notin T}{\operatorname{argmin}} d(\Re(Y), \Re(P_{T^{h-1} \cup \{i\}} Y))$ $I^h = \underset{I:I \subset \Omega \setminus I^{h-1}, |I|=K}{\operatorname{argmin}} \sum_{i=1}^{d} \sum_{j=1}^{Na} D^h(n_a)$ $T^h = T^{h-1} \cup \{(I^h - 1)d + 1 : I^h d\}$ $X^h = \underset{U:supp(U) \subseteq T}{\operatorname{argmin}} \|Y - \Phi U\|_F$ $R^h = Y - \Phi X^h$
End	
Output:	T^h and X^h

It can be seen from Table III that the JBMOLS algorithm proposed in this paper can successfully complete 1000 experiments when CR = 76%, which is much higher than the 67% compression rate required by the JBOMP algorithm. However, compared with the WJCS algorithm and the WL12M algorithm, there is still a certain gap. When CR = 80.5%, both WJCS algorithm and WL12M algorithm can successfully complete all reconstructions.

TABLE III
RECONSTRUCTION RATE OF EACH ALGORITHM UNDER DIFFERENT CR

CR/%	JBMOLS	WCJS	WL12M	JBOMP	BOMP	BOLS
85	0.006	0.832	0.769	0.002	0	0
83.5	0.249	0.909	0.874	0.156	0	0
82	0.735	0.994	0.986	0.451	0	0.001
80.5	0.949	1	1	0.66	0	0.007
79	0.994	1	1	0.841	0	0.025
77.5	0.999	1	1	0.913	0	0.083
76	1	1	1	0.97	0.003	0.172
74.5	1	1	1	0.982	0.021	0.318
73	1	1	1	0.984	0.097	0.461
71.5	1	1	1	0.997	0.272	0.631
70	1	1	1	0.997	0.443	0.692
68.5	1	1	1	0.995	0.615	0.803
67	1	1	1	1	0.735	0.86
65.5	1	1	1	1	0.811	0.893
64	1	1	1	1	0.88	0.926
62.5	1	1	1	1	0.917	0.942

It can be seen from Table IV that when $CR \ge 82\%$, the time

World Academy of Science, Engineering and Technology
International Journal of Information and Communication Engineering
Vol:17, No:6, 2023

required by the JBOMP algorithm is the least. When $CR <$ 82%, the running time required by the JBMOLS algorithm is less than that of the JBOMP algorithm. This is because the JBMOLS algorithm uses a threshold method to jump out. In the case of high CR, in order to meet the requirements of the algorithm reconstruction accuracy, the number of iterations is relatively large, so the time required exceeds the JBOMP algorithm. But with the increase of the CR, the JBMOLS algorithm performs better, which can save about 30% of the running time compared with the JBOMP algorithm. The WJCS algorithm and the WL12M algorithm are optimization algorithms, and their running time is two orders of magnitude higher than the greedy algorithm.

TABLE IV
RUNNING TIME OF EACH ALGORITHM UNDER DIFFERENT CR

CR/%	JBMOLS	WJCS	WL12M	JBOMP	BOMP	BOLS
85	0.2605	3.50	3.81	**0.1181**	0.1777	0.2828
83.5	0.2251	3.56	3.96	**0.1192**	0.1763	0.2830
82	0.1402	3.65	4.29	**0.1214**	0.1786	0.2823
80.5	**0.1079**	3.68	4.50	0.1312	0.1907	0.3005
79	**0.1008**	3.71	4.50	0.1372	0.1976	0.3125
77.5	**0.0976**	3.72	4.51	0.1346	0.1944	0.3085
76	**0.0970**	3.76	4.52	0.1360	0.1961	0.3115
74.5	**0.0886**	3.83	4.54	0.1255	0.1752	0.2784
73	**0.0913**	3.84	4.58	0.1289	0.1805	0.2864
71.5	**0.0911**	3.88	4.52	0.1265	0.1766	0.2834
70	**0.0915**	3.94	4.50	0.1287	0.1789	0.2857
68.5	**0.0924**	3.95	4.53	0.1301	0.1801	0.2892
67	**0.0936**	3.99	4.53	0.1286	0.1785	0.2875
65.5	**0.1009**	4.03	4.57	0.1336	0.1902	0.3017
64	**0.1022**	4.13	4.57	0.1367	0.1984	0.3125
62.5	**0.1023**	4.14	4.60	0.1374	0.1993	0.3172

In general, the optimization algorithm can complete the accurate reconstruction of the signal with a high compression rate, but the time required for this algorithm is too long, with an average running time of 3s-4s. The JBMOLS algorithm proposed in this paper is a greedy algorithm. Compared with the JBOMP algorithm, which is also a greedy algorithm, it has obvious advantages in terms of CR and running time required for accurate reconstruction. Compared with the two optimization algorithms, the average running time of the JBMOLS algorithm is only 0.1s, and when CR = 80.5%, JBMOLS achieves 94.9% reconstruction rate.

V. SUMMARIZE

In the application of WBANs for FECG signals, CS technology can improve energy utilization efficiency, but it must ensure that important information is not lost. In this paper, the JBMOLS algorithm is proposed. The success rate of this algorithm in the actual FECG signal transmission is close to the optimization algorithm. The JBMOLS algorithm is better than other greedy algorithms and takes less time. After comparative experiments, the proposed FECG signal compression transmission method combining Rbio5.5 wavelet, Bernoulli measurement matrix and JBMOLS algorithm can ensure short signal transmission and reconstruction process time and high

success rate.

For the sparse representation and compression of the signal, this paper only compares the existing wavelet basis and the existing measurement matrix through experimental simulation, and selects the Rbio5.5 wavelet and Bernoulli measurement matrix that are most suitable for FECG signal transmission. The next step should be to try to innovate in these two aspects to make it more suitable for WBANs hardware system for FECG remote monitoring.

REFERENCES

[1] S. Kumar, B. Deka and S. Datta, Weighted Block Compressed Sensing for Multichannel Fetal ECG Reconstruction, 2019 IEEE Region 10 Conference (TENCON). (2019) 2324-2328.
[2] D. L. Donoho, Compressed sensing, IEEE Transactions on Information Theory. 52(4) (2006) 1289-1306.
[3] Zhang Y C, Zhang W, Xu H Y, Epidemiological Aspects, Prenatal Screening and Diagnosis of Congenital Heart Defects in Beijing Frontiers in Cardiovascular Medicine. (2021).
[4] H. Mamaghanian, N. Khaled, D. Atienza and P. Vandergheynst, Compressed Sensing for Real-Time Energy-Efficient ECG Compression on Wireless Body Sensor Nodes, IEEE Transactions on Biomedical Engineering. 58(9) (2011) 2456-2466.
[5] M. Hasan, M. Reaz, M. Ibrahimy, M. Hussain, and J. Uddin, Detection and processing techniques of FECG signal for fetal monitoring, Biological procedures online. 11(1) (2009) 263–295
[6] J. Zhang, Z. L. Yu, Z. Gu, Y. Li and Z. Lin, Multichannel Electrocardiogram Reconstruction in Wireless Body Sensor Networks Through Weighted l1,2 Minimization, IEEE Transactions on Instrumentation and Measurement. 67(9) (2018) 2024-2034.
[7] Lu M, Chen W, Xia S, et al, Random Chirp Frequency-stepped Signal ISAR Imaging Algorithm Based on Joint Block-sparse Model ISAR, Journal of Electronics and Information Technology. 40(11) (2018) 2614-2620.
[8] Kumar S, Deka B, Datta S, Multichannel ECG Compression using Block-Sparsity-based Joint Compressive Sensing, Circuits Systems and Signal Processing. 39(12) (2020) 6299-6315.
[9] Zhang H P, Dong Z R, Wang Z, et al, CSNet: A deep learning approach for ECG compressed sensing, Biomedical Signal Processing and Control. 70 (2021).
[10] Qu Xin-chao, Zhang Yue, Real-time ECG compression algorithm based on compressed sensing, Computer Engineering and Design. 35(10) (2014) 3450−3454,3479.
[11] Mishra A, Thakkar F, Modi C, et al, Comparative analysis of wavelet basis functions for ECG signal compression through compressive sensing, International Journal of Computer Science and Telecommunications. 3(4) (2012) 23−31.
[12] R. Sameni, The open-source electrophysiological toolbox (OSET), 2012. (Online). Available: http://www.oset.ir
[13] Tropp J, Gilbert A C, Signal recovery form random measurements via orthogonal matching pursuit, IEEE Transactions on Information Theory. 53(12) (2007) 4655-4666.
[14] Zhang Y T, Liu C Y, Wei S S, et al, ECG quality assessment based on a kernel support vector machine and genetic algorithm with a feature matrix, Journal of Zhejiang University-Science C-Computers & Electronics. 15(7) (2014) 564-573.
[15] R. R. Naidu, P. Jampana and C. S. Sastry, Deterministic Compressed Sensing Matrices: Construction via Euler Squares and Applications, IEEE Transactions on Signal Processing. 64(14) (2016) 3566-3575.
[16] A. Elzanaty, A. Giorgetti and M. Chiani, Limits on Sparse Data Acquisition: RIC Analysis of Finite Gaussian Matrices, IEEE Transactions on Information Theory. 65(3) (2019) 1578-1588.
[17] Chen S, Billings S A, Luo W, Orthogonal least squares methods and their application to non-linear system identification, International Journal of contrl. 50(5) (1989) 1873-1896.
[18] H. F. Schepker and A. Dekorsy, Compressive Sensing Multi-User Detection with Block-Wise Orthogonal Least Squares, 2012 IEEE 75th Vehicular Technology Conference (VTC Spring). (2012) 1-5.
[19] J. Kim and B. Shim, Multiple Orthogonal Least Squares for Joint Sparse Recovery, 2018 IEEE International Symposium on Information Theory (ISIT), (2018) 61-65.

World Academy of Science, Engineering and Technology
International Journal of Information and Communication Engineering
Vol:17, No:6, 2023

[20] W. Dai and O. Milenkovic, Subspace Pursuit for Compressive Sensing Signal Reconstruction, IEEE Transactions on Information Theory. 55(5) (2009) 2230-2249.
[21] Wang L W, Wang X, Feng J F, Subspace distance analysis with application to adaptive Bayesian algorithm for face recognition, Pattern Recognition. 39(3) (2006) 456-464.
[22] Y. C. Eldar, P. Kuppinger and H. Bolcskei, Block-Sparse Signals: Uncertainty Relations and Efficient Recovery, IEEE Transactions on Signal Processing. 58(6) (2010) 3042-3054.